

引用格式: YE Lei, WANG Shun, YAO Zhonghui, et al. Mode-locked Fiber Laser Based on $\text{Ge}_2\text{Sb}_{1.5}\text{Bi}_{0.5}\text{Te}_5$ Saturable Absorber [J]. Acta Photonica Sinica, 2022, 51(4):0414001

叶蕾,王顺,姚中辉,等.基于 $\text{Ge}_2\text{Sb}_{1.5}\text{Bi}_{0.5}\text{Te}_5$ 可饱和吸收体的锁模光纤激光器[J].光子学报,2022,51(4):0414001

基于 $\text{Ge}_2\text{Sb}_{1.5}\text{Bi}_{0.5}\text{Te}_5$ 可饱和吸收体的锁模光纤激光器

叶蕾^{1,2},王顺²,姚中辉²,蒋成²,郭凯¹,张子暘²

(1 上海大学 材料科学与工程学院,上海 200444)

(2 中国科学院苏州纳米技术与纳米仿生研究所,江苏 苏州 215123)

摘 要: $\text{Ge}_2\text{Sb}_{1.5}\text{Bi}_{0.5}\text{Te}_5$ 薄膜具有宽光谱吸收和高稳定性的特点。在金镜上采用磁控溅射制备了 40 nm 厚的 $\text{Ge}_2\text{Sb}_{1.5}\text{Bi}_{0.5}\text{Te}_5$ 薄膜,将其在 150 °C 下退火 20 min,退火后 $\text{Ge}_2\text{Sb}_{1.5}\text{Bi}_{0.5}\text{Te}_5$ 由非晶态转变为晶态。测试发现晶态 $\text{Ge}_2\text{Sb}_{1.5}\text{Bi}_{0.5}\text{Te}_5$ 可饱和吸收体的调制深度提高到了原来的 1.4 倍,基于晶态 $\text{Ge}_2\text{Sb}_{1.5}\text{Bi}_{0.5}\text{Te}_5$ 可饱和吸收体实现了脉冲宽度为 1.52 ps、信噪比为 47 dB 的光纤锁模激光器。制备了 40、60、80 nm 的 $\text{Ge}_2\text{Sb}_{1.5}\text{Bi}_{0.5}\text{Te}_5$ 薄膜,分析表明,随着 $\text{Ge}_2\text{Sb}_{1.5}\text{Bi}_{0.5}\text{Te}_5$ 薄膜厚度的增加,光吸收率明显增加,这说明 $\text{Ge}_2\text{Sb}_{1.5}\text{Bi}_{0.5}\text{Te}_5$ 薄膜的光学性质具有可控性, $\text{Ge}_2\text{Sb}_{1.5}\text{Bi}_{0.5}\text{Te}_5$ 材料在超快激光器中有应用潜力。

关键词: $\text{Ge}_2\text{Sb}_{1.5}\text{Bi}_{0.5}\text{Te}_5$; 可饱和吸收体; 锁模; 掺铒; 光纤激光器; 退火

中图分类号: TN248

文献标识码: A

doi: 10.3788/gzxb20225104.0414001

0 引言

由于光纤激光器具有较高的电-光和光-光转换效率、可变的波长范围、高质量的输出光束、结构紧凑、成本低等特点,同时受益于光纤器件的成熟,近年来得到了迅速发展,它成为了激光领域的研究热点^[1-4]。光纤激光器优异的特性使其在材料加工、生物医学、工业生产、军事安全等领域有着广泛的应用,例如精密加工、激光雕刻、医疗器械精密切割等^[5-6]。超快光纤激光器是在光纤激光器的基础上利用锁模器件来实现超短脉冲的输出。与连续光光纤激光器相比,其最显著的特点是极窄的脉冲宽度,可达皮秒甚至飞秒量级。超快光纤激光器的面世为超快光谱学、高带宽光通信、材料精密加工、超快动力学过程等研究翻开了全新的篇章^[7-9]。超快光纤激光器主要通过主动锁模和被动锁模的方式来实现。主动锁模是在谐振腔内放置一个振幅或相位调制器,通过外部信号周期性的调节其损耗或者光程,从而实现锁模脉冲序列。被动锁模是在谐振腔内放置一个可饱和吸收体(Saturable Absorber, SA),基于 SA 对激光的非线性可饱和效应来实现锁模脉冲序列的输出。相对于主动锁模,被动锁模由于可实现更窄的脉冲输出,结构紧凑以及易于操作等优势,得到了更多的关注^[10-11]。而 SA 的调制深度、饱和通量等参数是决定激光器输出性能的关键。因此研究人员在不断探寻性能优异的可饱和吸收体材料。

近年来,研究人员基于材料本身的特性已经发现了许多可应用于超快激光器的可饱和吸收体材料,如碳纳米管、石墨烯、黑磷等具有宽光谱响应的材料^[12-17]。目前商用可饱和吸收体多为半导体可饱和吸收反射镜,但是其存在外延结构复杂、成本高以及有限的工作窗口等因素制约着其发展。碳纳米管、石墨烯等这些

基金项目: 国家自然科学基金(No.61875222)

第一作者: 叶蕾(1997—),女,硕士研究生,主要研究方向为近红外半导体材料和器件的研制。Email: lye2020@sinano.ac.cn

导师(通讯作者): 张子暘(1975—),男,研究员,博士,主要研究方向为半导体光电子材料和器件的研制、光子集成器件的研制、低维材料的分子数外延生长研究。Email: zy Zhang2014@sinano.ac.cn

郭凯(1983—),男,教授,博士,主要研究方向为热电材料设计、性能调控策略、热稳定性改善及热电器件组装。Email: kai.guo@shu.edu.cn

收稿日期: 2022-01-04; 录用日期: 2022-03-08

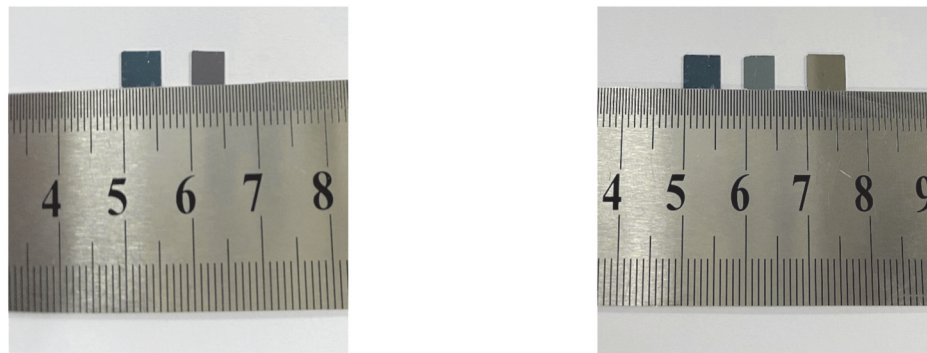
<http://www.photon.ac.cn>

纳米材料损伤阈值较低且在实际应用中存在可靠性低等缺点。黑磷对周围环境十分敏感,空气中的水分、氧气等都会影响材料本身的性质。因此,研究人员也在通过不断探索出更多可利用的材料和优化现有材料的性能来进一步拓宽光纤激光器应用的道路^[18]。Ge₂Sb_{1.5}Bi_{0.5}Te₅(GSBT)材料不仅具有宽的光谱响应,较高的热、化学和机械稳定性,而且可以通过调控温度实现非晶态和晶态的快速转变,因此能够结合激光直写技术在其表面制备微纳结构来进一步去调控表面光场,优化其光学特性^[19-20]。GSBT材料已经作为一种杰出的抗蚀剂被研究者们频繁地应用于激光直写纳米制备技术中,但是它在光子学领域的研究还处于起步阶段,研究者们尚未关注到GSBT材料在超快光纤激光器中的应用。对GSBT材料的光学特性及其应用的探索,不仅促进了对该材料的全面认识,也可以有效地推动基于GSBT的光学器件的发展。

本文研究了退火前后GSBT的光学特性,采用退火修饰,使其调制深度由2.7%提升到了3.8%,将其作为SA构建了环形腔超快激光器,获得了脉冲宽度为1.52 ps、信噪比为47 dB的锁模激光脉冲。为了进一步探究GSBT在超快激光器中的应用,制备了不同厚度的GSBT-SA,随着厚度的增大,GSBT-SA的光吸收率逐渐提升。

1 GSBT样品的制备

首先,采用电子束蒸发技术在GaAs衬底上沉积400 nm的金作为反射镜。然后,将GSBT靶材和GaAs/Au衬底分别固定于磁控溅射的源位置和样品位置,磁控溅射的工作压力为0.1 Pa、功率为50 W、Ar流量为25 sccm(standard cubic centimeter per minute),首次溅射时间为690 s,通过台阶仪测量厚度为40 nm,溅射速率为0.058 nm/s。GSBT作为一种常见的无机相转变材料,可以利用热效应改变材料晶相,因此采用真空管式退火炉对厚度为40 nm的GSBT-SA进行退火,退火条件和退火时间为150 °C和20 min,退火前后的GSBT薄膜的照片如图1(a)所示。为了探究厚度变化对材料性能的影响,利用磁控溅射分别溅射了1 000 s、1 380 s得到了厚度约为60、80 nm的GSBT薄膜,如图1(b)所示,从左至右分别为厚度为40、60、80 nm的GSBT薄膜的照片。采用X射线衍射分析仪(X-Ray Diffraction analyzer, XRD)研究退火对GSBT晶相的影响,并用分光光度计测定GSBT其材料的吸收光谱。



(a) GSBT films before (left) and after (right) annealing

(b) GSBT films with thickness of 40, 60 and 80 nm (from left to right)

图1 GSBT薄膜实物图

Fig.1 GSBT films pictures

2 锁模光纤激光器系统的搭建

搭建了光纤激光器系统来测试退火后40 nm GSBT样品作为SA的输出特性。图2为光纤激光器系统图,中心波长为980 nm的半导体激光器(Laser Diode, LD)作为泵浦源来保证谐振腔内有足够的泵浦能量,然后与980/1 550 nm的波分复用器(Wavelength Division Multiplexer, WDM)相连。截取不同长度的掺铒光纤(Er-Doped Fiber, EDF)作为增益介质,通过对比增益介质后端的输出功率,确定最终的增益介质长度为1.3 m。偏振无关隔离器(Polarization-Independent Isolator, PI-ISO)能使信号光沿着固定的方向导通而在其他方向损耗,保证了信号光在腔内的单向运转。偏振控制器(Polarization Controller, PC)用来调节腔内偏振态使其具有相同的相位延迟,产生相位叠加从而影响锁模状态,通过调整偏振控制器的角度,获得最佳

的锁模激光器的输出特性。光束经过环形器(Circulator, CIR)作用于可饱和吸收体上,GSBT可饱和吸收体放置在一个铜基座上,环形器的一端尾纤的光纤跳线头通过螺丝旋钮于基座上方,入射光垂直照射在SA上,最终通过环形器的另一端重新耦合回环形腔。为了减少谐振腔内能量损耗,实验时通过精细调控旋钮螺丝,获得最佳的光束入射角度。随后腔内激光脉冲通过分束比为90:10的输出耦合器(Output Coupler, OC),其中10%端口输出的激光被用来实时观测该激光的性能,90%的激光被用来继续在腔内循环震荡。激光器的时域特性由数字示波器(Keysight DSOS054A)测量,脉冲的光谱特性使用光谱分析仪(Anritsu MS9740A)测量,射频频谱分析仪(Keysight N9322C)测量脉冲序列的重复频率和频谱特性,脉冲宽度利用自相关仪(Femtochrome FR-103XL)测量。

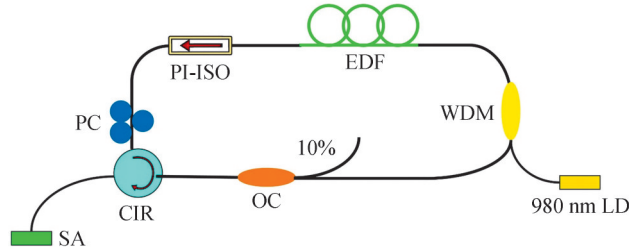


图2 光纤激光器系统示意图
Fig.2 Schematic diagram of fiber laser system

3 结果与讨论

无机相转变材料GSBT可以通过热效应改变其材料晶相,进而调控材料的性能。为了证实退火前后GSBT样品的晶相,对其进行XRD表征,如图3所示,未退火的GSBT样品没有明显的结晶峰,说明未退火的GSBT样品呈现典型的非晶态(aGSBT)特征,而经过150℃下的退火修饰之后,(200)晶面的衍射峰出现在29.5°附近,这证实了GSBT由非晶态转变为晶态(cGSBT)。图4是测量的aGSBT和cGSBT样品在1300~1600 nm波长范围内的吸收光谱。从图中可以看出在测试波长范围内cGSBT样品的吸收率明显大于aGSBT的吸收率,在1550 nm处的吸收率分别为5.61%和21.16%,这说明GSBT样品结晶后对光的吸收能力有所增强。

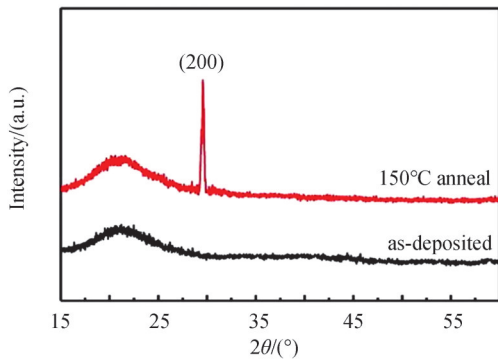


图3 退火前后的GSBT薄膜的XRD图
Fig.3 XRD images of GSBT films before and after annealing

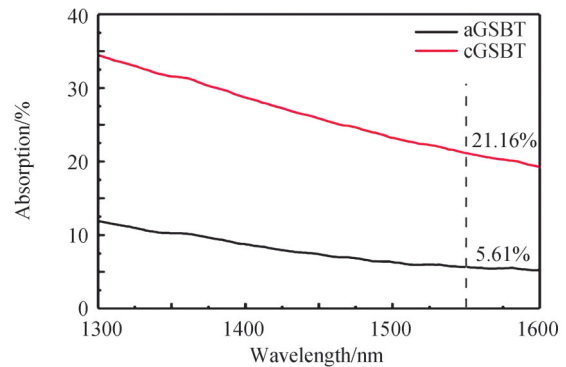


图4 aGSBT和cGSBT薄膜的吸收光谱
Fig.4 Absorption spectra of aGSBT and cGSBT

为了探索aGSBT-SA和cGSBT-SA的非线性吸收特性,利用双臂法非线性测试系统对其进行测试。图5是退火前后GSBT样品的非线性传输特性曲线,它反映了输入光功率与透射率之间的对应关系,通过式(1)拟合后得到的。

$$T(I) = 1 - \Delta T \exp\left(-\frac{I}{I_{\text{sat}}}\right) - T_{\text{ns}} \quad (1)$$

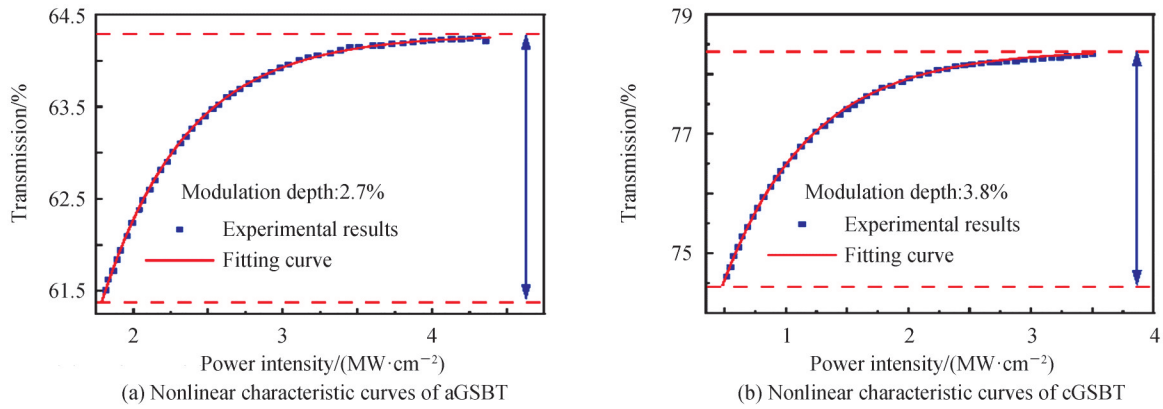
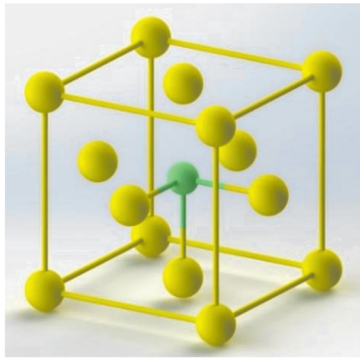
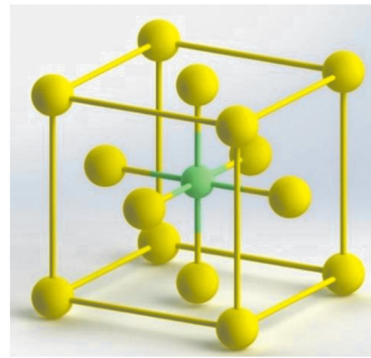


图5 GSBT薄膜的非线性特性曲线
Fig.5 Nonlinear characteristic curves of GSBT films

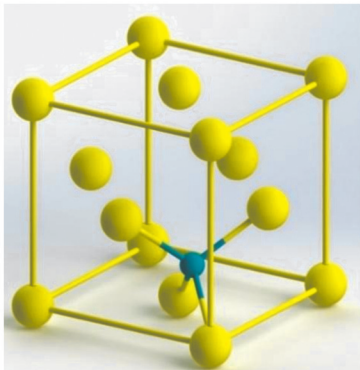
式中, $T(I)$ 、 ΔT 、 I 、 I_{sat} 和 T_{ns} 分别是透射率、调制深度、输入光强、入射饱和光强和非饱和损耗。通过拟合退火前 aGSBT-SA 的调制深度为 2.7%, 退火后 cGSBT-SA 的调制深度增加至 3.8%, 非饱和损耗也从 35.7% 降至 21.6%。退火后 cGSBT-SA 的非线性吸收能力提升的主要原因是未退火的 aGSBT 薄膜中大量不饱和键以及缺陷的存在, 使其内部局域缺陷态密度高。退火后, aGSBT 形成了长程有序的结构, 不饱和键减少, 局域缺陷态减少, 对光的吸收增多, 更容易达到饱和状态^[21-22]。Ge₂Sb_{1.5}Bi_{0.5}Te₅ (GSBT) 是通过在 Ge₂Sb₂Te₅ (GST) 中掺杂少量的 Bi 获得的, Bi 原子在 GST 中选择性地替换了部分 Sb 原子^[23]。退火前 GSBT 的整体结构比较复杂, 从局部来看, Sb(Bi) 原子位于由 3 个 Sb-Te 键形成的直角三棱锥中的一个顶点处(图 6(a)), Ge 原子位于由 4 个 Ge-Te 键构成的四面体中心处(图 6(c))。而退火后形成的晶态 GSBT 是类似于 NaCl 型的面心立方结构, 它的(111)晶面被 Te-Sb-Te-Ge 原子依次占据, 其原子结构示意图如图 6(e)所示。Sb(Bi) 原子、Ge 原子分别位于由 6 个 Sb-Te 键形成八面体结构的中心(图 6(b))和由 6 个 Ge-Te 键构成的八面体中心(图 6(d)), cGSBT 整体形成了稳定的结构^[24]。另一方面, 非晶态 GST 的带隙为 0.7 eV, 晶态 GST 的带隙降为 0.5 eV^[25], 因此 GSBT 转变为晶态之后带隙也会相对减小。带隙的减小使得激子的结合



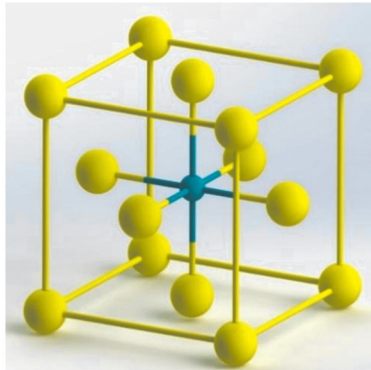
(a) Local configuration of Sb (Bi) atoms in aGSBT



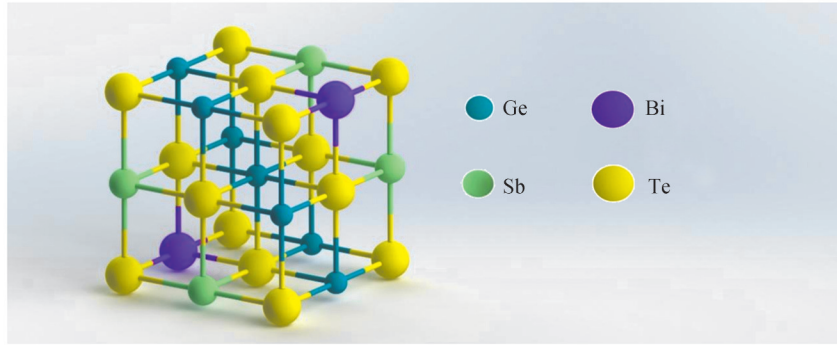
(b) Local configuration of Sb (Bi) atoms in cGSBT



(c) Local configuration of Ge atoms in aGSBT



(d) Local configuration of Ge atoms in cGSBT



(e) Atomic arrangement model of cGSBT

图6 GSBT中的各原子排列

Fig.6 Atomic arrangement of GSBT

能也越小。结合能较低的激子,其电子空穴对的复合效率更慢,而材料的调制深度与电子空穴对的复合效率成反比。因此,带隙更小的cGSBT,其电子空穴对复合效率更慢,则调制深度越大,非线性吸收特性越优异。

将cGSBT-SA集成到图2所示的锁模光纤激光器系统中来获得锁模激光脉冲,激光器输出如图7所示。从图7(a)中可以看出,锁模激光器的输出功率随泵浦功率的增加而增加,当泵浦功率增加至192.6 mW时,输出光功率达最大值3.831 mW,斜率效率为2.2%。图7(b)是激光器输出的时域脉冲序列,锁模脉冲间隔为291 ns,由此可见,基于cGSBT可饱和吸收体的锁模激光器有稳定的脉冲输出。图7(c)为锁模输出光谱,可以看出其中心波长为1557 nm,3dB带宽为3.21 nm。输出脉冲的频谱图如图7(d)所示,可以得到脉冲重复频率为3.44 MHz,从图7(e)可以看出信噪比为47 dB,说明锁模脉冲工作在一个相对稳定的状态。图7(f)为锁模激光器的单脉冲形状,自相关仪测得的单脉冲轨迹通过高斯拟合后得到脉冲宽度为1.52 ps。时间带宽积公式为

$$\text{TBP} = \tau \cdot c \cdot \frac{\Delta\lambda}{\lambda_c^2} \quad (2)$$

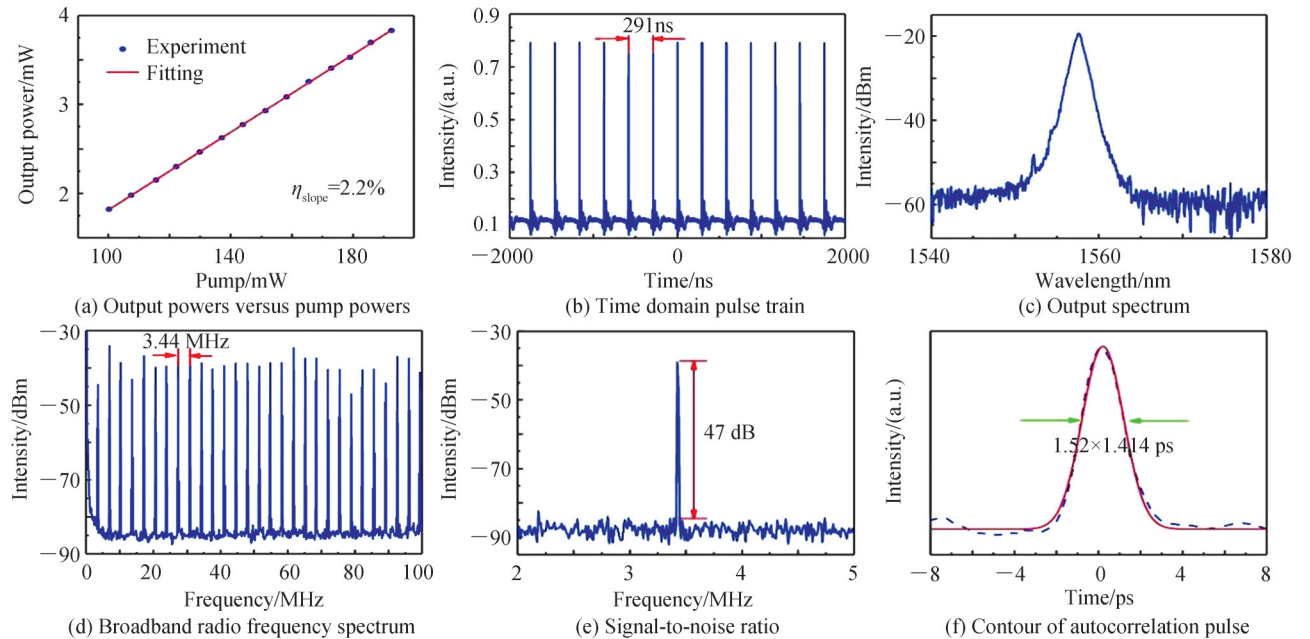


图7 基于cGSBT可饱和吸收体的锁模激光器的输出特性

Fig.7 Output characteristics of the mode-locked laser based on cGSBT saturable absorber

式中, τ 为脉冲持续时间, c 为光速, $\Delta\lambda$ 为 3 dB 带宽, λ_0 是中心波长。计算可得激光脉冲的时间带宽积为 0.604。每隔 5 h 测量了激光器的输出光谱, 在 360 h 的稳定性测试时间范围内, 锁模激光器的中心输出波长没有明显漂移, 光谱 3 dB 宽度保持稳定。

cGSBT-SA 的激光器输出特性证实了其在超快激光领域的应用潜力。为了进一步研究薄膜厚度对 GSBT 吸收特性的影响, 分别测试了 60、80 nm 厚的 GSBT 薄膜的光吸收率。如图 8 所示, 随着厚度的增加, GSBT 薄膜在 1550 nm 波长处的光吸收率逐渐增加, 分别是 40.44% 和 52.28%。因此, GSBT 作为一种潜在的可饱和吸收体材料, 可以通过退火、增加膜厚等简单的方式来提升激光器输出特性。

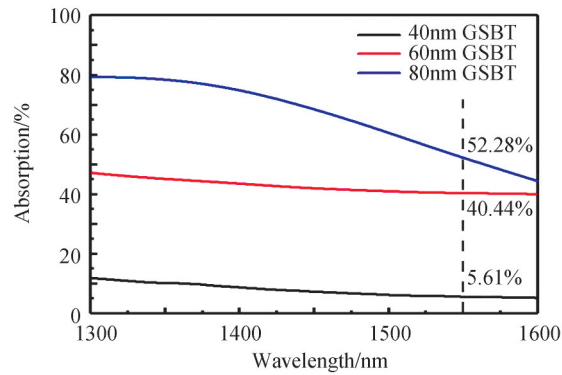


图 8 40、60、80 nm 的 GSBT 的吸收光谱
Fig.8 Absorption spectra of GSBT films of 40, 60, 80 nm

4 结论

采用磁控溅射制备了 40 nm 的 aGSBT 薄膜, 通过退火使其转变为 cGSBT 薄膜, 有效地减少了局域缺陷态、减小了带隙, 使其调制深度提升至 3.8%。基于 cGSBT-SA 构建了锁模激光器, 实现了中心波长为 1557 nm、重复频率为 3.44 MHz、脉冲宽度为 1.52 ps、信噪比 47 dB 的激光输出。除此之外, 研究了薄膜厚度对 GSBT 的吸收特性的影响, 发现增加厚度也是 GSBT 薄膜增强光吸收的一个可行的方法。GSBT 材料有望成为应用于锁模光纤激光器的可饱和吸收体材料的候选者。

参考文献

- [1] NISHIZAWA N. Ultrashort pulse fiber lasers and their applications[J]. Japanese Journal of Applied Physics, 2014, 53(9): 090101.
- [2] LIN Y H, LIN S F, CHI Y C, et al. Using n- and p-type Bi₂Te₃ topological insulator nanoparticles to enable controlled femtosecond mode-locking of fiber lasers[J]. ACS Photonics, 2015, 2(4): 481-490.
- [3] FERMAN M E, HARTL I. Ultrafast fiber laser technology [J]. IEEE Journal of Selected Topics in Quantum Electronics, 2009, 15(1): 191-206.
- [4] JIANG Cheng, NING Jiqiang, LI Xiaohui, et al. Development of 1550 nm InAs/GaAs quantum dot saturable absorber mirror with a short period superlattice capping structure towards femtosecond fiber laser application[J]. Nanoscale Research Letters, 2019, 14(1): 362.
- [5] KAFKA J D, BAER T, HALL D W. Mode-locked erbium-doped fiber laser with soliton pulse shaping [J]. Optics Letters, 1989, 14(22): 1269-1271.
- [6] SHI Wei, FANG Qiang, ZHU Xiushan, et al. Fiber lasers and their applications[J]. Applied Optics, 2014, 53(28): 6554-6568.
- [7] KELLER U. Recent developments in compact ultrafast lasers[J]. Nature, 2003, 424(6950): 831-838.
- [8] NELSON L E, JONES D J, TAMURA K, et al. Ultrashort-pulse fiber ring lasers[J]. Applied Physics B, 1997, 65(2): 277-294.
- [9] DING Jianyi, LU Baole, WANG Kaile, et al. Wavelength tunable dissipative soliton mode-locked fiber laser based on nonlinear amplifier loop mirror[J]. Acta Photonica Sinica, 2021, 50(7): 0714002.
丁建一, 陆宝乐, 王凯乐, 等. 基于非线性放大环的波长可调谐耗散孤子锁模光纤激光器[J]. 光子学报, 2021, 50(7): 0714002.
- [10] YAO Jian, YAO Jianping, WANG Yong, et al. Active mode-locking of tunable multi-wavelength fiber ring laser[J]. Optics Communications, 2001, 191(3): 341-345.

- [11] ZIRNGIBL M, STULZ L W, STONE J, et al. 1.2 ps pulses from passively mode-locked laser diode pumped Er-doped fiber ring laser[J]. Electronics Letters, 1991, 27(19): 1734-1735.
- [12] NICHOLSON J W, WINDELER R S, DIGIOVANNI D J. Optically driven deposition of single-walled carbon-nanotube saturable absorbers on optical fiber end-faces[J]. Optics Express, 2007, 15(15): 9176-9183.
- [13] XIA Fengnian, WANG Han, XIAO Di, et al. Two-dimensional material nanophotonics[J]. Nature Photonics, 2014, 8(12): 899-907.
- [14] JIANG Cheng, WANG Xu, LIU Jian, et al. Realization of high-performance tri-layer graphene saturable absorber mirror fabricated via a one-step transfer process[J]. Journal of Semiconductors, 2020, 41(1): 012302.
- [15] JIANG Cheng, WANG Xu, WANG Hongpei, et al. Tunable graphene/quantum-dot van der waals heterostructures' saturable absorber plane arrays by two-step femtosecond and nanosecond laser postprocessing[J]. Advanced Photonics Research, 2021, 3(1): 2100183.
- [16] ZHAO Yang, GUO Penglai, LI Xiaohui, et al. Ultrafast photonics application of graphdiyne in the optical communication region[J]. Carbon, 2019, 149: 336-341.
- [17] LAN Dongfang, CHENG Tonglei, QU Yuhuan, et al. Tungsten carbide nanoparticles as saturable absorber for q-switched erbium-doped fiber laser[J]. IEEE Photonics Technology Letters, 2022, 34(2): 113-116.
- [18] DENG Haiqin, FAN Chao, GUO Kun, et al. Research of fiber pulse laser generation with oblique grown PbSe nanosheets saturable absorber (Invited) [J]. Acta Photonica Sinica, 2021, 50(10): 1014002.
邓海芹,樊超,郭琨,等. 基于斜立生长硒化铅纳米片可饱和吸收体的光纤脉冲激光研究(特邀)[J]. 光子学报, 2021, 50(10): 1014002.
- [19] LI Jianzheng, ZHANG Jianming, ZHANG Haoran, et al. A high-selective positive-type developing technique for phase-change inorganic resist $\text{Ge}_2\text{Sb}_{2(1-x)}\text{Bi}_{2x}\text{Te}_5$ [J]. Materials Science in Semiconductor Processing, 2015, 40: 690-694.
- [20] XI Hongzhu, LIU Qian, GUO Shengming. Phase change material $\text{Ge}_2\text{Sb}_{1.5}\text{Bi}_{0.5}\text{Te}_5$ possessed of both positive and negative photoresist characteristics[J]. Materials Letters, 2012, 80: 72-74.
- [21] ULAŞ K, MUSTAFA Y, H. GUL Y, et al. The effect of thickness and/or doping on the nonlinear and saturable absorption behaviors in amorphous GaSe thin films[J]. Journal of Applied Physics, 2010, 108(6): 063102.
- [22] LIU Jing, WEI Jingsong. Optical nonlinear absorption characteristics of AgInSbTe phase change thin films[J]. Journal of Applied Physics, 2009, 106(8): 083112.
- [23] WANG Heng, DAI Yang, HUANG Jianping, et al. Research on fabrication of memristor by femtosecond laser based on $\text{Ge}_2\text{Sb}_{2-x}\text{Bi}_x\text{Te}_5$ ($x=0, 0.2$) material[J]. Journal of Integration Technology, 2019, 8(6): 48-64.
王恒,戴阳,黄建平,等. 飞秒激光制备基于 $\text{Ge}_2\text{Sb}_{2-x}\text{Bi}_x\text{Te}_5$ ($x=0, 0.2$) 材料忆阻器的研究[J]. 集成技术, 2019, 8(6): 48-64.
- [24] LI Jianzheng, ZHENG Lirong, LIU Qian, et al. A study on inorganic phase-change resist $\text{Ge}_2\text{Sb}_{2(1-x)}\text{Bi}_{2x}\text{Te}_5$ and its mechanism[J]. Physical Chemistry Chemical Physics, 2014, 16(40): 22281-22286.
- [25] LEE B S, ABELSON J R., BISHOP S G, et al. Investigation of the optical and electronic properties of $\text{Ge}_2\text{Sb}_2\text{Te}_5$ phase change material in its amorphous, cubic, and hexagonal phases[J]. Journal of Applied Physics, 2005, 97(9): 093509.

Mode-locked Fiber Laser Based on $\text{Ge}_2\text{Sb}_{1.5}\text{Bi}_{0.5}\text{Te}_5$ Saturable Absorber

YE Lei^{1,2}, WANG Shun², YAO Zhonghui², JIANG Cheng², GUO Kai¹, ZHANG Ziyang²

(1 School of Materials Science and Engineering, Shanghai University, Shanghai 200444, China)

(2 Suzhou Institute of Nano-Tech and Nano-Bionics, Chinese Academy of Sciences, Suzhou, Jiangsu 215123, China)

Abstract: Fiber lasers have a wide range of applications in material processing, biomedical, industrial production, military security and other fields with high electrical-optical and optical-optical conversion efficiency, variable wavelength range, high quality of output beam, compact structure, and low cost, which becomes the research hotspot in recent years. Fiber lasers with the ultrafast laser pulse are mainly realized by active mode-locking and passive mode-locking methods. Compared with the active mode-locking technology, the passive mode-locking has attracted more attention on account of its advantages such as narrower pulse output, compact structure and convenient operation, in which saturable absorber is the core component. The modulation depth and saturation fluence of saturable absorbers determines the output characteristics of passively mode-locked lasers. Therefore, it is necessary to explore excellent saturable absorbent materials. $\text{Ge}_2\text{Sb}_{1.5}\text{Bi}_{0.5}\text{Te}_5$ materials have a wide spectral response, high thermal,

chemical and mechanical stability, and can achieve rapid transition between amorphous and crystalline states at low temperature. $\text{Ge}_2\text{Sb}_{1.5}\text{Bi}_{0.5}\text{Te}_5$ materials have been frequently used in laser direct writing technology as an outstanding photoresist, but its research in the field of photonics is still in its infancy. To our best knowledge, $\text{Ge}_2\text{Sb}_{1.5}\text{Bi}_{0.5}\text{Te}_5$ materials have not been used as the saturable absorber for the generation of the ultrafast laser pulse. Therefore, the exploration of optical properties and applications of $\text{Ge}_2\text{Sb}_{1.5}\text{Bi}_{0.5}\text{Te}_5$ could promote the comprehensive understanding of $\text{Ge}_2\text{Sb}_{1.5}\text{Bi}_{0.5}\text{Te}_5$ materials and effectively drive the development of optical devices based on $\text{Ge}_2\text{Sb}_{1.5}\text{Bi}_{0.5}\text{Te}_5$ materials. Here, $\text{Ge}_2\text{Sb}_{1.5}\text{Bi}_{0.5}\text{Te}_5$ films with the thickness of 40 nm were prepared by the magnetron sputtering method on a gold mirror under the atmospheric pressure of 0.1 Pa, the power of 50 W and the Ar flow of 25. Then the $\text{Ge}_2\text{Sb}_{1.5}\text{Bi}_{0.5}\text{Te}_5$ films were annealed at 150 °C for 20 min in vacuum tube annealing furnace. X-ray diffraction analysis of $\text{Ge}_2\text{Sb}_{1.5}\text{Bi}_{0.5}\text{Te}_5$ films shows that the as-grown $\text{Ge}_2\text{Sb}_{1.5}\text{Bi}_{0.5}\text{Te}_5$ films are amorphous and after annealing the crystalline state has been observed in $\text{Ge}_2\text{Sb}_{1.5}\text{Bi}_{0.5}\text{Te}_5$ films. The optical absorption of crystalline $\text{Ge}_2\text{Sb}_{1.5}\text{Bi}_{0.5}\text{Te}_5$ films in the range of 1 300~1 600 nm is significantly higher than that of amorphous $\text{Ge}_2\text{Sb}_{1.5}\text{Bi}_{0.5}\text{Te}_5$ films, and the absorbance of amorphous and crystalline $\text{Ge}_2\text{Sb}_{1.5}\text{Bi}_{0.5}\text{Te}_5$ films at 1 550 nm are 5.61% and 21.16% measured by spectrophotometer, respectively. A typical balanced twin-detector test system is used to explore the nonlinear absorption characteristics of amorphous and crystalline $\text{Ge}_2\text{Sb}_{1.5}\text{Bi}_{0.5}\text{Te}_5$ saturable absorber. The modulation depth of the amorphous $\text{Ge}_2\text{Sb}_{1.5}\text{Bi}_{0.5}\text{Te}_5$ saturable absorber is 2.7% and that of crystalline $\text{Ge}_2\text{Sb}_{1.5}\text{Bi}_{0.5}\text{Te}_5$ after annealing increases to 3.8%, which is 1.4 times higher than the amorphous $\text{Ge}_2\text{Sb}_{1.5}\text{Bi}_{0.5}\text{Te}_5$ saturable absorber. The reason for the improved nonlinear absorption capacity of crystalline $\text{Ge}_2\text{Sb}_{1.5}\text{Bi}_{0.5}\text{Te}_5$ films can be mainly attributed to the formation of the long-range ordered structure with less unsaturated bonds and less local defects in the crystalline $\text{Ge}_2\text{Sb}_{1.5}\text{Bi}_{0.5}\text{Te}_5$ saturable absorber. Moreover, the crystalline $\text{Ge}_2\text{Sb}_{1.5}\text{Bi}_{0.5}\text{Te}_5$ saturable absorber also exhibits the smaller band gap which decreases the binding energy of excitons. The lower binding energy of excitons slows the recombination efficiency of electron hole pairs, and the modulation depth of saturable absorber is inversely proportional to the recombination efficiency of electron hole pairs. Therefore, crystalline $\text{Ge}_2\text{Sb}_{1.5}\text{Bi}_{0.5}\text{Te}_5$ with a smaller band gap has a greater modulation depth. Based on the crystalline $\text{Ge}_2\text{Sb}_{1.5}\text{Bi}_{0.5}\text{Te}_5$ saturable absorber, an Er-doped fiber laser system has been constructed to obtain the ultrafast laser pulse in which a semiconductor laser with a central wavelength of 980 nm is used as the pump source and is connected to a wavelength division multiplexer at 980/1 550 nm. A 1.3 m Erbium-doped fiber is employed as the gain medium. The polarization independent isolator ensures the unidirectional operation of the signal light in the cavity, and the polarization controller is used to adjust the polarization state in the cavity to affect the mode-locked state. The laser beam is applied to saturable absorber through the ring device and re-coupled back to the ring cavity to generate a mode-locked laser pulse. Then the laser pulse passes through a fiber coupler with a beam splitter ratio of 90:10. 10% of the output laser is used to observe the performance of the laser in real time, and the remaining 90% of the laser is used to continue oscillating in the cavity. The obtained output pulse width is 1.52 ps, the repetition frequency is 3.44 MHz, and the signal-to-noise ratio is 47 dB. In addition, to investigate the effect of film thickness on the absorption properties, $\text{Ge}_2\text{Sb}_{1.5}\text{Bi}_{0.5}\text{Te}_5$ films of 60 and 80 nm were prepared by magnetron sputtering. The experimental results of the UV-Vis-NIR absorption spectra show that the optical absorption increases with the increase of $\text{Ge}_2\text{Sb}_{1.5}\text{Bi}_{0.5}\text{Te}_5$ films thickness, which indicates the controllability of optical properties of $\text{Ge}_2\text{Sb}_{1.5}\text{Bi}_{0.5}\text{Te}_5$ films and reveals the great potential of $\text{Ge}_2\text{Sb}_{1.5}\text{Bi}_{0.5}\text{Te}_5$ materials in ultrafast lasers. Our finding can provide reference for the application of phase transition materials in photonics and help for the wide application of fiber lasers.

Key words: $\text{Ge}_2\text{Sb}_{1.5}\text{Bi}_{0.5}\text{Te}_5$; Saturable absorber; Mode-locked; Erbium-doped; Fiber lasers; Anneal

OCIS Codes: 140.4050; 160.4760; 190.7110; 320.5390